Cluster observations of lower hybrid turbulence within thin layers at the magnetopause

A. Vaivads,[1] M. André,[1] S. C. Buchert,[1] J.-E. Wahlund,[1] A. N. Fazakerley,[2] and N. Cornilleau-Wehrlin[3]

Received 10 July 2003; revised 3 September 2003; accepted 22 October 2003; published 4 February 2004.

[1] We use data from the Cluster satellites to study waves in the frequency range of ~2–150 Hz at the magnetopause. In addition to broad band wave turbulence we identify lower hybrid drift waves and whistler waves. Wave amplitudes maximize within narrow current sheets that are associated with density gradients and electron beams and that can be the separatrices of the reconnection. The dispersion properties of lower hybrid drift waves are studied using interferometric measurements of electric field. A direct estimate of the wave role in the particle diffusion across the magnetopause shows that their importance is limited only to the narrow current sheet. *INDEX TERMS:* 2724 Magnetospheric Physics: Magnetopause, cusp, and boundary layers; 2772 Magnetospheric Physics: Plasma waves and instabilities; 7859 Space Plasma Physics: Transport processes; 7863 Space Plasma Physics: Turbulence. **Citation:** Vaivads, A., M. André, S. C. Buchert, J.-E. Wahlund, A. N. Fazakerley, and N. Cornilleau-Wehrlin (2004), Cluster observations of lower hybrid turbulence within thin layers at the magnetopause, *Geophys. Res. Lett.*, *31*, L03804, doi:10.1029/2003GL018142.

1. Introduction

[2] Observations of the magnetopause starting from early missions of ISEE 1 and ISEE 2 have shown that the magnetopause is a region of increased wave activity often of a broadband character [*Gurnett et al.*, 1979]. The waves have frequencies from below the proton gyrofrequency f_{cH+} up to the upper hybrid frequency. Part of this turbulence can have wide spectral peaks near the lower hybrid frequency f_{LH} [*André et al.*, 2001]. These waves have been explained as originating from the lower hybrid drift instability (LHDI) at density and magnetic field gradients within the magnetopause [*Gary and Eastman*, 1979]. It has been proposed that lower hybrid drift waves can contribute to the particle diffusion across the magnetopause and be a source of anomalous resistivity [*Treumann et al.*, 1991].

[3] Turbulent electric fields with frequencies near f_{LH} at plasma boundaries similar to the magnetopause have been seen also in numerical simulations and laboratory experiments [*Rogers et al.*, 2000; *Carter et al.*, 2002]. It has been shown that these waves are due to LHDI. The turbulence development has been extensively studied, e.g., along the separatrices of the reconnection X-line [*Rogers et al.*, 2000], and its role for the development of reconnection and wave-particle interactions is a topic of many recent simulation studies. Laboratory reconnection experiments show that LHDI fluctuations do not play essential role in the determination of the reconnection rate [*Carter et al.*, 2002]. Similar conclusion was reached in a recent study of the diffusion region crossing by the Polar spacecraft [*Bale et al.*, 2002]. However, numerical simulations show that the lower hybrid drift waves can help in forming of the narrow current sheets necessary for the explosive onset of the reconnection [*Scholer et al.*, 2003]. More studies are necessary to resolve the importance of the wave turbulence and particularly waves near the lower hybrid frequency.

[4] In this article we study waves at frequencies around f_{LH} and above for one particular magnetopause crossing where the four Cluster satellites were run in a mode that allowed high time resolution observations of waves and particles.

2. Observations

[5] We study a high latitude, northern hemisphere, dayside magnetopause crossing, MLT ~14, seen by the Cluster spacecraft at 2002-02-06 0811:57 UT. The spacecraft separation was ~100 km, Figure 1. The magnetopause normal $\mathbf{n}_{MP}$ is obtained from times at which spacecraft see the magnetopause density gradient. s/c 1 and 4 are closest to being on the same flux tube, with ~20 km distance between their flux tubes. s/c 3 is the last to cross the magnetopause while s/c 1, 2 and 4 cross shortly one after the other.

[6] We use electric field E and probe potential with respect to the spacecraft p1, p2, p3 and p4 data from the EFW instrument and the magnetic field data from FGM and STAFF instruments [*Escoubet et al.*, 1997 and references therein]. Figure 2 shows an overview of the event. Figures 2a and 2b show the plasma density n_{Vps}(estimated from the probe to spacecraft potential) and **B**; the magnetopause is the region between ~0811:50 UT and ~0812:40 UT. Detailed observations from the region marked by yellow, where the largest amplitude electric field turbulence is observed, are shown in Figures 2c–2l. Plasma beta during the crossing is ~0.3–0.5. The overall structure of this region is studied in the accompanying paper by *André et al.* [2004], while here we concentrate on the wave observations.

[7] *André et al.* [2004] shows that the largest electric fields on scales between c/ω_{pe} and c/ω_{pi} (electron and ion inertial lengths) are also seen in the region marked by yellow in Figures 2a and 2b. The region of strong electric fields coincides with a narrow layer density gradient and

[1]Swedish Institute of Space Physics, Uppsala, Sweden.
[2]Mullard Space Science Laboratory, University College London, United Kingdom.
[3]Centre d'étude des Environnements Terrestre et Planétaires, CNRS, France.

0094-8276/04/2003GL018142

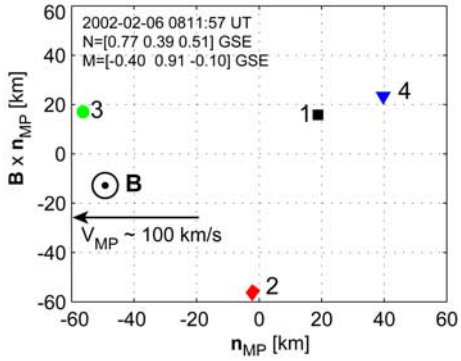

Figure 1. Spacecraft configuration.

strong currents and it is speculated that it can be associated with the separatrix of the reconnection region. It also coincides with the inner boundary of the magnetopause separating regions with and without high energy plasma sheet electrons. Within the same region we observe wave turbulence with the highest electric field amplitudes.

[8] Figure 2c shows the density as seen by all four s/c, s/c 4 has higher time resolution due to the internal burst mode of EFW instrument. The small scale density structure is similar between s/c 1 and 4, which are on almost the same flux tube, while it differs from s/c 2 and 3 which are ~80 km away (c/ω_{pi}~180 km). Also, the narrow density gradients are not oriented exactly parallel to the magnetopause because the time difference at which s/c observe the small density gradients is not the same as expected from Figure 1. The changes in By, Figure 2d, are associated with field aligned currents. The strongest parallel currents from gradient in B_Y are observed at s/c 1 and 4. They are associated with e- beams parallel to **B** [*André et al.*, 2004]. The increase in |**B**|, Figure 2e, at all spacecraft is associated with the density decrease. For s/c 1 and 4 the strongest parallel currents, the density gradient and the change in the magnetic field magnitude all coincide. Such agreement is not so obvious for s/c 2 and 3. Figures 2f–2i show E measurements high-pass filtered at 180 Hz. S/c 1 had only one operational probe pair and therefore only one component of E in the spin plane is available. For s/c 1 and 4 it is seen that the strongest wave activity coincides with the density and magnetic field gradients (for waves E~50 mV/m corresponds to $|E|^2/\varepsilon_0 nkT \sim 10^{-5}$). Figures 2j–2l shows the wavelet spectra of **E**, **B** and field-aligned Poynting flux (it is obtained from the spectra of E and B and is related to the group velocity of waves) for s/c 4. **E** and **B** spectra have a broadband character with sometimes clear

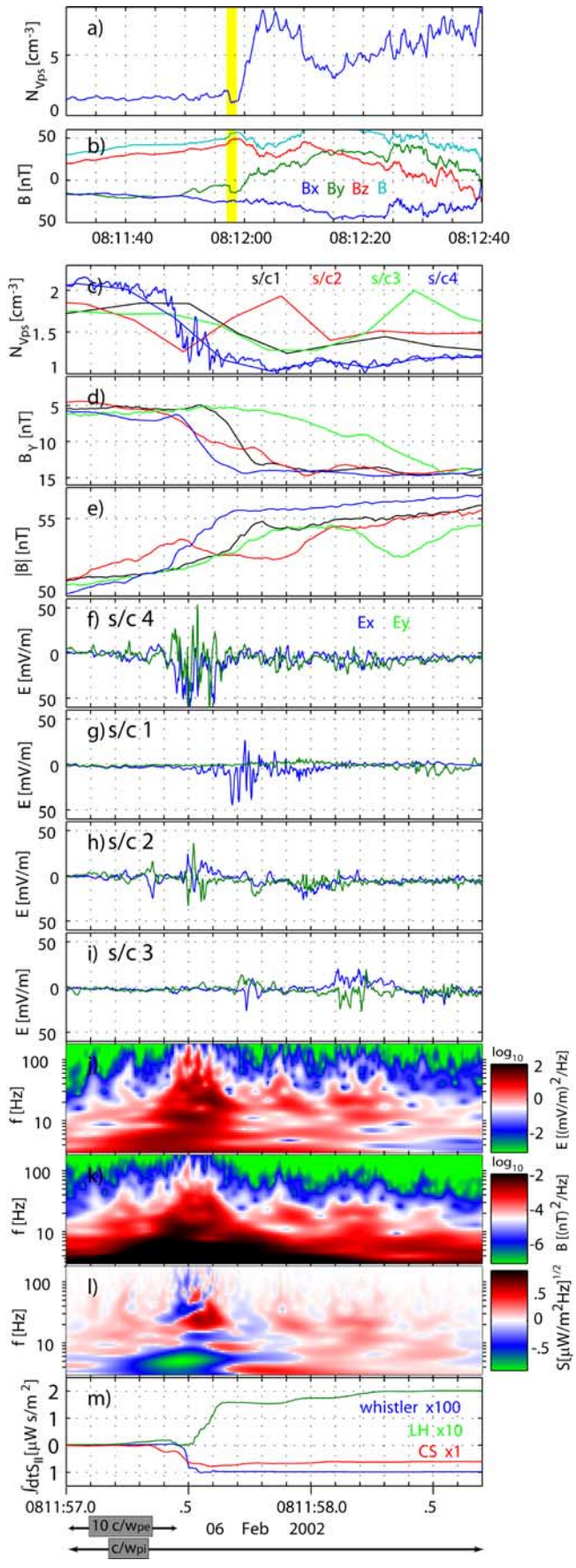

Figure 2. Overview plot of the magnetopause crossing. (a) s/c4 n_{Vps}, (b) s/c4 **B** GSE, yellow marks interval that is zoomed in (c)-(m), (c) n_{Vps}, (d) B_Y GSE, (e) |**B**|, (f-(i), E in the s/c spin plane (approx. GSE X,Y), (j) s/c4 E spectrogram (sum of two measured components), (k) s/c4 B spectrogram (sum of all components), (l) s/c4 field-aligned Poynting flux spectrogram, (m) integrated Poynting flux estimated from fields band-pass filtered over frequency intervals 80–150 Hz(whistler), 15–35 Hz(lower hybrid LH), 3–8 Hz(current sheet CS), the resultant flux has been multiplied by a factor shown inside figure. The inertial length scales of the electrons and ions are marked.

peaks near f_{LH} frequency. Also within the region of highest wave amplitudes there is a narrow region in time at ~0811:57.5 UT where there is a peak at ~100 Hz, typical whistler frequency. In this frequency range whistler wave emissions are seen also deeper in the magnetosphere. However, at the magnetopause the emissions are located in a much more narrow region, are more electrostatic, and propagate at large angle with respect to **B**. Figure 2m shows, for s/c 4, the integrated field-aligned Poynting flux in three different frequency intervals, low frequency interval that corresponds to the time scale of the narrow current sheet, the frequency interval near f_{LH} and the whistler frequency interval. In all frequency ranges there is a significant energy flux right within the narrow current sheet. The energy flux is largest in the low frequency range while it is a factor of hundred lower in the whistler frequency region. The Poynting flux of the waves near f_{LH} is preferentially parallel to **B**, i.e. in the same direction as electrons carrying the parallel current of the narrow current layer *André et al.* [2004]. The whistler waves on the other hand propagate antiparallel to the magnetic field. In all frequency intervals s/c 4 sees larger energy fluxes than s/c 2 and 3 (s/c 1 is not used for Poynting flux estimates).

[9] We study in more detail waves with frequencies near f_{LH} as these waves have high amplitude during the event (several tens of mV/m), they have been observed earlier at the magnetopause and are often discussed in the context of reconnection and as a possible source of plasma diffusion across the magnetopause. On s/c 4 we can perform interferometry measurements to derive dispersion properties of these waves. **B** is at large angle (45–50 degrees) with respect to the spin plane, which allows a good estimate of the phase velocity perpendicular to **B**. We filter data in the lower hybrid frequency range, 15–35 Hz, and look at the phase difference between the two pairs of signals, p1–p3 vs p4–p2 and p2–p3 vs p4–p1. We obtain several values of the phase velocity within one wave cycle by correlating the steepest gradients, as well as maxima and minima of the two signals.

[10] Figure 3 shows the results of the interferometric analysis. Figure 3b shows electric field measurements from p1–p3 and p2–p3 (the signals from opposite pairs are almost identical and therefore only one is shown). Waves with largest amplitude are at the density gradient as discussed earlier. In Figure 3c we show in the magnetopause oriented reference frame the components of the inverse phase velocity (proportional to wave number) as obtained from the interferometry. The correction due to the magnetopause motion has been applied. Phase velocity is of the order 100 km/s but large variations are seen in the phase velocity even on the scale of a few wave lengths. The estimate of the inverse wave length in the satellite spin plane is shown in Figure 3d. Typical wave lengths are of the order 5 km. This is a few times the electron gyroradius ρ_e (ρ_e ~1 km for T_e = 250 eV) or approximately the same as c/ω_{pe} (c/ω_{pe} ~4 km for n = 1.5 cm^{-3}).

[11] Assuming that the spacecraft potential variations are due to the density variations we can make an observational estimate of the electron transport across the magnetopause due to the waves. Figure 3e shows density fluctuations dn, obtained filtering n_{Vps} in the lower hybrid frequency range. Using filtered electric field E_f data, Figure 3b, we can construct the fluctuating drift velocity $\mathbf{v}_f = \mathbf{E}_f \times \mathbf{B}/B^2$, assuming that $\mathbf{E}_f \cdot \mathbf{B} = 0$. Here $\mathbf{v}_f$ corresponds to the electron drift due to the wave electric field. Electron flux across the magnetopause due to the waves, $dn\mathbf{v}_f \cdot \mathbf{n}_{MP}$, is shown in Figure 3f. It is seen that the flux is largest where the wave amplitude maximize and that there is consistent flow in the direction of the magnetopause normal, from the magnetosphere towards the magnetosheath (antiparallel to the local density gradient). Using the estimate of the background density gradient at the place of highest amplitude waves we can express the electron flux in units of the diffusioncoefficient, m^2/s (the diffusion coefficient $D = \langle dn\mathbf{v}_f \cdot \mathbf{n}_{MP} \rangle / \nabla \langle n_{Vps} \rangle$ would be an average over at least one wave length). The value one obtains is ~10^9 m^2/s.

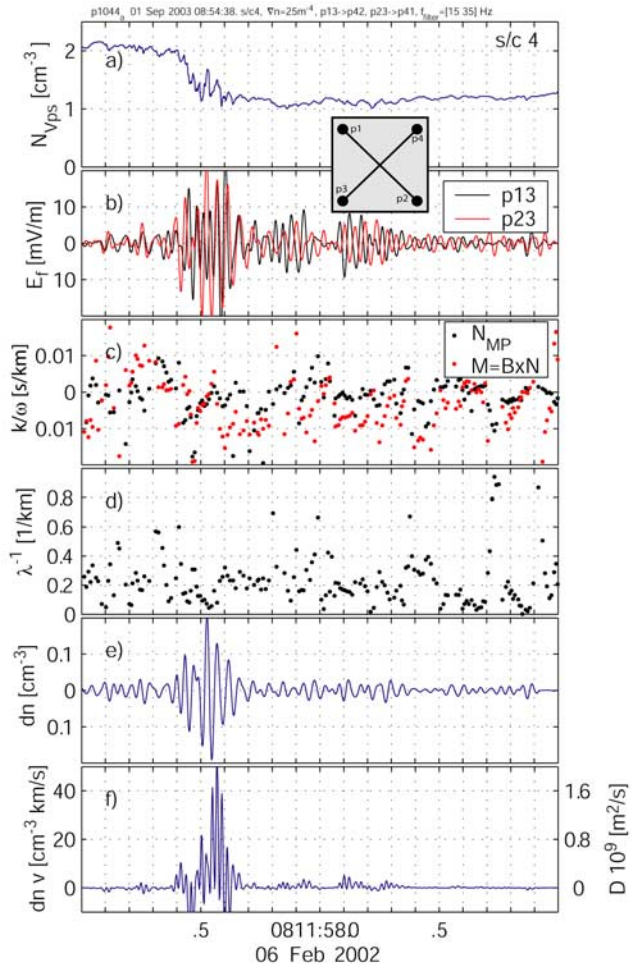

Figure 3. (a) n_{Vps}, (b) electric field between p1 and p3, p2 and p3 band-pass filtered 15–35 Hz, inset shows the location of probes (c) the components of the inverse phase velocity along n_{MP} and perpendicular to it, (d) inverse wave length, (e) n_{Vps} fluctuations, band-pass filtered 15–35 Hz, (f) electron flux across the magnetopause, the axes on the right gives the estimate of D assuming density gradient 25 m^{-4}.

3. Results and Discussion

[12] We have studied in detail a magnetopause crossing during which the Cluster spacecraft were at short separation (~100 km, of the order of half c/ω_{pi}) and the internal burst of the electric field instrument on s/c4 allowed detailed analysis

of the wave turbulence. The results show that waves with highest amplitude electric fields are concentrated to a narrow current sheet associated with a density gradient and a strong current having components both parallel and perpendicular to **B**. The waves show broad-band spectra, however, spectral peaks at the lower hybrid frequency and at higher frequencies (whistlers) can be distinguished. The fact that wave amplitude decreases fast outside the current sheets and that satellites that observe the largest currents (s/c 4 and 1) see the largest amplitude fluctuations indicates that the waves are most probably generated within the regions of strongest current and damp as they propagate along and/or across the magnetic field lines.

[13] More detailed analysis of the waves in the lower hybrid frequency range show their wave length to be of the order of c/ω_{pe} or a few ρ_e. This is consistent with the waves being lower hybrid drift waves, analytical estimates predict the largest growth at $k_\perp \rho_e \sim 1$. While lower hybrid drift waves are believed to be generated by the density gradients, the free energy source of the waves can also be an electron beam associated with the parallel current. Several facts support this. First, waves around the lower hybrid frequency carry energy preferentially in the same direction as the electron beam carrying parallel current. Secondly, energy flux carried by electrons along B is measured to be $\sim$55 $\mu W/m^2$ that is more than enough to generate the energy flux $\sim$ 1$\mu W/m^2$ of the waves in the lower hybrid frequency range. Also recent reconnection simulations show the possibility of lower hybrid wave generation by electron beams along the separatrices from the reconnection line *Drake et al.* [2003].

[14] The generation mechanism for waves in the whistler frequency region is probably different as they propagate opposite to the electron beam. Anisotropy or loss-cone instabilities are possible candidates.

[15] Lower hybrid waves have been also used to explain plasma transport across the magnetopause. Here we could make an observational estimate of the electron transport across the current layer due to the waves near f_{LH}. Before analyzing the result there are a few important things to note. First, even though the satellite potential depends on both the electron density and temperature, we used it as an estimate of plasma density fluctuations because theory predicts it to be less sensitive to temperature variations. Secondly, the velocity that we obtain is not the total electron velocity but only the $\mathbf{E}_f \times \mathbf{B}$ part. However, it should be close to the total plasma velocity as electrons are weakly magnetized (wave lengths are several ρ_e). The result in Figure 3f shows that the electron flow due to waves is preferentially from the magnetosphere into the magnetosheath (opposite to the local density gradient), the maximum electron flow is $\sim$ 30 cm^{-3}km/s. Outside the narrow current layer the flow due to the waves is practically negligible. If we assume that the transport process is a diffusion process we can estimate the diffusion coefficient using the value of the background density gradient within the region of highest amplitude waves, $\sim$25 m^{-4}. The value we obtain is slightly below 10^9 m^2/s. This is often used as a lower limit needed for significant transport across the magnetopause. For E$\sim$20 mV/m, the obtained value of diffusion coefficient is close to theoretical estimates based either on quasi-linear theory [*Treumann et al.*, 1991] or nonlinear modulational instability [*Shapiro et al.*, 1994]. Here we show that the transport due to waves with frequencies near f_{LH} is only important across the narrow current layer and not across the entire magnetopause.

[16] It is interesting to note that most of the turbulence and lower hybrid wave properties that we describe above are similar to the observations in laboratory reconnection experiments [*Carter et al.*, 2002]. Here strongest fluctuations are confined to the low-beta edge of the current sheets (corresponding to magnetosphere side of the magnetopause), $k\rho_e \sim 1$, wave spectra show broadband character with spectral peaks near the lower hybrid frequency, and the wave correlation length is small. However, the relation of waves to narrow current sheets, the presence of whistlers, as well as energy and plasma transport requires further laboratory studies.

[17] *André et al.* [2004] speculates that the narrow current sheet is related to the separatrices of the reconnection line. From simulations it is known that separatrices are regions of large wave activity and strong parallel and perpendicular currents. It is a place of significant energy conversion at the magnetopause and the understanding of waves there and plasma transport across separatrices is of highest interest. This study has dealt with only one such case.

[18] **Acknowledgments.** We thank S. Bale, A. I. Eriksson, A. Lahiff, C. Moukis, A. Pedersen, A. Tjulin, and R. Wilson for valuable discussions and help in preparation and interpretation of data. AV research is supported by the Swedish Research Council.

References

André, M., A. Vaivads, S. Buchert, A. Fazakerley, and A. Lahiff (2004), Thin electron-scale layers at the magnetopause, *Geophys. Res. Lett.*, *31*, L03803, doi:10.1029/2003GL018137.

André, M., et al. (2001), Multi-spacecraft observations of broadband waves near the lower hybrid frequency at the earthward edge of the magnetopause, *Annales Geophysicae*, *19*, 1471–1481.

Bale, S. D., F. S. Mozer, and T. Phan (2002), Observation of lower hybrid drift instability in the diffusion region at a reconnecting magnetopause, *Geophys. Res. Lett.*, *29*(24), 2180, doi:10.1029/2002GL016113.

Carter, T. A., M. Yamada, H. Ji, R. M. Kulsrud, and F. Trintchouk (2002), Experimental study of lower-hybrid drift turbulence in a reconnecting current sheet, *Phys. of Plasmas*, *9*, 3272.

Drake, J. F., M. Swisdak, C. Cattell, M. A. Shay, B. N. Rogers, and A. Zeiler (2003), Formation of Electron Holes and Particle Energization During Magnetic Reconnection, *Science*, *299*, 873–877.

Escoubet, C. P., R. Schmidt, and M. L. Goldstein (1997), Cluster — Science and Mission Overview, *Space Science Reviews*, *79*, 11–32.

Gary, S. P., and T. E. Eastman (1979), The lower hybrid drift instability at the magnetopause, *J. Geophys. Res.*, *84*, 7378–7381.

Gurnett, D. A., R. R. Anderson, B. T. Tsurutani, E. J. Smith, G. Paschmann, G. Haerendel, S. J. Bame, and C. T. Russell (1979), Plasma wave turbulence at the magnetopause — Observations from ISEE 1 and 2, *J. Geophys. Res.*, *84*, 7043–7058.

Rogers, B. N., J. F. Drake, and M. A. Shay (2000), The onset of turbulence in collisionless magnetic reconnection, *J. Geophys. Res.*, *27*(19), 3157–3160.

Scholer, M., I. Sidorenko, C. H. Jaroschek, R. A. Treumann, and A. Zeiler (2003), Onset of collisionless magnetic reconnection in thin current sheets: Three-dimensional particle simulations, *Phys. Plasmas*, *10*, 3521–3527.

Shapiro, V. D., V. I. Shevchenko, P. J. Cargill, and K. Papadopoulos (1994), Modulational instability of lower hybrid waves at the magnetopause, *J. Geophys. Res.*, *99*(A12), 23,735–23,740.

Treumann, R. A., J. Labelle, and R. Pottelette (1991), Plasma diffusion at the magnetopause — The case of lower hybrid drift waves, *J. Geophys. Res.*, *96*(A9), 16,009–16,013.

A. Vaivads, M. André, S. C. Buchert, and J.-E. Wahlund, Swedish Institute of Space Physics, Box 537, SE-751 21 Uppsala, Sweden. (andris@irfu.se)

A. N. Fazakerley, Mullard Space Science Laboratory, University College London, United Kingdom.

N. Cornilleau-Wehrlin, Centre d'étude des Environnements Terrestre et Planétaires, CNRS, France.